This is a preliminary version of the article published as:
M. Chaves and J.-L. Gouzé, Acta Biotheoretica, 58(2), pp. 217-232, 2010.

Comparing Boolean and piecewise affine differential models for genetic networks

Madalena Chaves[1] Laurent Tournier[2] Jean-Luc Gouzé[1]

[1]INRIA, project-team COMORE, 2004 Route des Lucioles, BP 93, 06902 Sophia Antipolis, France
[2]INRA, Unité de Mathématique, Informatique et Génôme (UR 1077) Domaine de Vilvert, 78350 Jouy-en-Josas, France
Emails: madalena.chaves@inria.fr,laurent.tournier@jouy.inra.fr,jean-luc.gouze@inria.fr

Abstract

Multi-level discrete models of genetic networks, or the more general piecewise affine differential models, provide qualitative information on the dynamics of the system, based on a small number of parameters (such as synthesis and degradation rates). Boolean models also provide qualitative information, but are based simply on the structure of interconnections. To explore the relationship between the two formalisms, a piecewise affine differential model and a Boolean model are compared, for the carbon starvation response network in *E. coli*. The asymptotic dynamics of both models are shown to be quite similar. This study suggests new tools for analysis and reduction of biological networks.

1 Introduction

Genetic regulatory networks have been analysed through various different formalisms, in particular continuous differential models (von Dassow et al, 2000), piecewise affine (PWA) models (Ropers et al, 2006; Grognard et al, 2007; Chaves et al, 2006), multi-level discrete models (Thomas and D'Ari, 1990; Sánchez and Thieffry, 2001), and Boolean models (Glass and Kauffman, 1973; Glass, 1975; Chaves et al, 2009; Tournier and Chaves, 2009). Each formalism has its advantages and drawbacks, and the combination of different methods may provide complementary information on the system. In this study the Boolean and PWA formalisms are compared. Many computational tools are available for the analysis of Boolean models: these can also be used to study PWA systems, by transforming the continuous system into a discrete system. We propose an algorithmic method to construct a Boolean model from a piecewise affine model: first, the PWA system gives rise to a multi-level discrete system, where each variable takes values in a finite set; then the discrete model can be translated into a Boolean model, by appropriately extending the state space as in, for instance, van Ham (1979) (see Section 2 and Appendix 1).

To illustrate this point of view, we will analyse the PWA model of the carbon starvation response in *E.coli* developed in Ropers et al (2006), which was studied mathematically in Grognard et al (2007). The Boolean model has two attractors that correctly represent the asymptotic behaviour of the piecewise linear system, under two different input conditions. Following the method developed in Tournier and Chaves (2009), it is possible to identify a family of "operational interactions" for each attractor: a subset of the original network of interactions that actively contribute to characterize the dynamics within that attractor. This family of operational interactions, together with the components involved, constitutes a smaller (Boolean) subsystem of the original system, which can be used to construct a reduced model of the system of differential equations. The asymptotic dynamics of the PWA and Boolean models agree in most qualitative aspects (Section 4). In particular, we illustrate the correspondance between a sliding mode in the PWA model (Grognard et al, 2007) - which may induce chattering or Zeno behaviour (Zhang et al, 2001) in one of the variables,- and period 2 oscillations in the Boolean model (see Section 5). These results suggest future applications of Boolean network analysis to model reduction techniques.

2 Piecewise affine, discrete and Boolean models for genetic networks

To compare the results of discrete and Boolean modelling frameworks, we first discuss a method to transform a model from one formalism to the other without changing the dynamical behaviour. Throughout the paper, for a system with $n > 0$ variables, let x_i $(i = 1,\ldots,n)$ denote the continuous variables, V_i the corresponding discrete variables, each with a discrete set of values $V_i \in \{0,1,\ldots,d_i\}$ $(d_i \geq 1)$. Below we will define also $V_{i,j}$ $(j = 1,\ldots,d_i)$, to be the Boolean variables associated to the multi-level variable V_i.

2.1 From discrete to Boolean models

One way to construct a Boolean (purely binary) model from a discrete (multi-level) model is to generate a set of binary variables for each multi-level variable (see, for instance, van Ham (1979); Snoussi and Thomas (1993); Thomas and D'Ari (1990)), satisfying some properties, as stated in H1 and H2 below.

Consider a discrete model $\Sigma_d = (\Omega_d, F_d)$, with variables $V = (V_1,\ldots,V_n)$, state space $\Omega_d = \{0,1,\ldots,d_1\} \times \cdots \times \{0,1,\ldots,d_n\}$, and a map $F_d : \Omega_d \to \Omega_d$ which defines the state transition table. This map lists all the possible transitions from each state, and thus defines the possible dynamical trajectories of the system. At each state $V \in \Omega_d$, the next possible value for variable i is given by: $V_i^+ = (F_d)_i(V)$. Throughout this paper we will consider only *asynchronous dynamics*, and assume that exactly one variable is updated at any given time (for more details, see Appendix 1). Thus, the updating rule satisfies:

$$V^+ \in \{W \in \Omega_d : \ \exists k \text{ s.t. } W_k = (F_d)_k(V) \neq V_k \text{ and } W_j = V_j, \ \forall j \neq k \ \}. \tag{1}$$

Following previous work on multi-level systems (Snoussi and Thomas, 1993; Thomas and D'Ari, 1990), it will be assumed that the state transitions satisfy:

H1. Each variable V_i can only switch from its current level to an immediately adjacent level, that is: $V_i^+ \in \{V_i - 1, V_i, V_i + 1\}, \ \forall i$.

In other words, any variable V_i can only be increased or decreased by one unit at each time. This hypothesis represents the continuity of the biological variables: the concentration of a given protein cannot evolve from level d to level $d+2$ without passing through level $d+1$.

To construct a Boolean model Σ_b associated to Σ_d, the state space will be expanded by adding extra variables. If a discrete variable V_m takes values in the set $\{0,1,\ldots,d_m\}$, then, in the Boolean model, d_m variables will be created:

H2. For each $V_m \in \{0,1,\ldots,d_m\}$ in the discrete model, generate $V_{m,1},\ldots,V_{m,d_m} \in \{0,1\}$ such that:

$$V_m = k \Leftrightarrow [\ V_{m,1} = \cdots = V_{m,k} = 1 \text{ and } V_{m,k+1} = \cdots = V_{m,d_m} = 0\ ]. \tag{2}$$

In particular, note that $V_{m,k} \geq V_{m,k+1}$, for all $k = 1,\ldots,d_m - 1$, meaning that if V_m is at a certain level, then all inferior levels must be "filled" as well. This hypothesis requires special attention when constructing the Boolean model, since we will wish to avoid transitions from a *permissible* (i.e., satisfying H2) to a *forbidden* (i.e., not satisfying H2) state. Our procedure deals with this problem in a natural way (see Appendix 1), and guarantees that no transitions from permissible to forbidden states take place.

2.2 From piecewise affine to multi-level discrete models

In models of genetic regulatory networks it is common to represent the activation (or inhibition) of one gene by another by a Heaviside function, that is, if the concentration of the first "gene" is below a certain threshold, then there is no transcription of the second gene; while above that threshold transcription is fully turned on. This description gives rise to *piecewise affine differential models* (Glass and Kauffman, 1973; Glass, 1975). Let θ_i^* represent the threshold for the activation (resp., inhibition) of x_k by x_i, and define:

$$s^+(x_i,\theta_i^*) = \begin{cases} 0, & x_i < \theta_i^* \\ 1, & x_i > \theta_i^*, \end{cases}$$

(resp., $s^-(x_i,\theta_i^*) = 1 - s^+(x_i,\theta_i^*)$)[1]. These functions are not defined at the threshold points. At these points, the system of equations is defined as a differential inclusion (Gouzé and Sari, 2002; Casey et al, 2006). To construct a multi-level discrete model from the PWA model, based on the work of Thomas and D'Ari (1990), we will consider that the number of levels of a given variable x_i, is equal to the number of thresholds which define the influence of x_i on the other variables:

$$0 < \theta_i^1 < \theta_i^2 < \cdots < \theta_i^{d_i} < +\infty.$$

Define the corresponding multi-level discrete variable by:

$$V_i = \begin{cases} 0, & 0 \le x_i \le \theta_i^1 \\ k, & \theta_i^k < x_i \le \theta_i^{k+1}, \ \ k = 1,\ldots,d_i-1 \\ d_i, & \theta_i^{d_i} < x_i < +\infty. \end{cases} \tag{3}$$

To obtain a transition table (F_d) for the discrete model, the ordering among thresholds is used. Let V_i and V_i^+ denote, respectively, the discrete current and updated values for the continuous variable x_i. The PWA equation for x_i will take a particular expression for each V (see (5)-(8), for an example), and have a corresponding focal point $\hat{x} = \hat{x}(V)$. Then V_i is updated to evolve towards $\hat{x}_i$, in such a way that hypothesis H1 is satisfied: if $\hat{x}_i$ is in the interval $(\theta_i^k, \theta_i^{k+1})$, then

$$V_i^+ = (F_d)_i(V) \begin{cases} \min\{d_i, V_i+1\}, & V_i < k, \\ V_i, & V_i = k, \\ \max\{0, V_i-1\}, & V_i > k. \end{cases} \tag{4}$$

The state transition table F_d for the discrete system associated to the PWA system can thus be built. The discrete system evolves according to an asynchronous strategy, following the updating rule (1).

3 Example: the carbon starvation response in *E.coli*

As an example, the *E. coli* model developed by Ropers *et al.* in Ropers et al (2006) and studied in Grognard et al (2007) will be analysed (see these two references for more details on the biological and modelling aspects). This model describes the dynamics of a family of genes that regulate the carbon starvation response in *E.coli* (Fig. 1): *crp* (x_c), *cya* (x_y), *fis* (x_f), *gyrAB* (x_g), *topA* (x_t), and *rrn* (x_r). Nutritional stress is represented by an input $u \in \{0,1\}$: $u = 0$ if carbon is present (no stress), and $u = 1$ in the absence of carbon.

The vector $x = (x_c, x_y, x_f, x_g, x_t)' \in \mathbb{R}^5_{\ge 0}$ denotes the continuous variables, $V = (C, Y, F, G, T)' \in \Omega_d$ denotes the corresponding multi-level discrete variables, and C_i, $i = 1,\ldots,d_c$ denote the Boolean variables, associated with *crp* (similar notation is used for the other network components). The PWA equations are taken from Ropers et al (2006) and shown in Table 1. To construct a discrete (multi-level) system from the model in Table 1, note that:

- *crp* contributes to *fis* inhibition and its own activation once it reaches threshold θ_c^1; contributes to *cya* inhibition at θ_c^3. Since threshold θ_c^2 doesn't enter into any equations, it will not be considered here;
- *cya* contributes to *fis* inhibition and *crp* activation at θ_y^1; contributes to its own inhibition at θ_y^3. As before, the level θ_y^2 will not be considered here;
- *gyrAB* contributes to *fis* activation at θ_g^1; inhibits itself and activates *topA* at θ_g^2;
- *topA* influences *gyrAB* and inhibits itself at θ_t^1; contributes to *fis* inhibition at θ_t^2;
- *fis* has five threshold concentrations. It inhibits *crp* promoters 1 and 2 once it reaches lower thresholds θ_f^1 and θ_f^2, activates *rrn* at threshold θ_f^3, inhibits gyrAB and activates topA at θ_f^4, and inhibits itself at θ_f^5.

[1]The superscripts "+" or "-" indicate whether the step function is increasing or decreasing. This notation is not related to V^+ used in discrete and Boolean systems, which designates the successor of state V. Since s^+ and V^+ are used for different systems (respectively, PWA and discrete), the notations will not be confused.

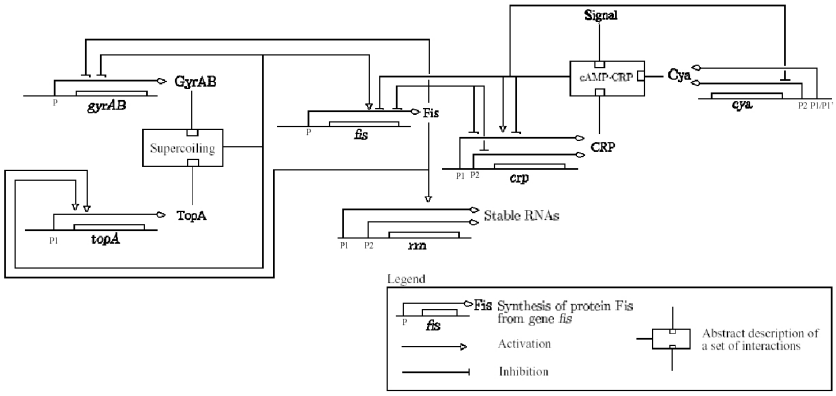

Figure 1: Genetic network, including proteins and regulations that come into play during a nutritional stress response in *E.coli*: CRP activation module (Cya, CRP, Fis), DNA Topology module (GyrAB, TopA, Fis), stable RNA output module (Rrn).

Table 1: Piecewise affine model and parameter inequalities.

$$
\begin{aligned}
\dot{x}_c &= \kappa_c^1 + \kappa_c^2 s^-(x_f,\theta_f^2)s^+(x_c,\theta_c^1)s^+(x_y,\theta_y^1)s^+(u,\theta_u) + \kappa_c^3 s^-(x_f,\theta_f^1) - \gamma_c x_c \\
\dot{x}_y &= \kappa_y^1 + \kappa_y^2[1 - s^+(x_c,\theta_c^3)s^+(x_y,\theta_y^3)s^+(u,\theta_u)] - \gamma_y x_y \\
\dot{x}_f &= \kappa_f^1[1 - s^+(x_c,\theta_c^1)s^+(x_y,\theta_y^1)s^+(u,\theta_u)]s^-(x_f,\theta_f^5) \\
&\quad + \kappa_f^2 s^+(x_g,\theta_g^1)s^-(x_t,\theta_t^2)s^-(x_f,\theta_f^5) \times [1 - s^+(x_c,\theta_c^1)s^+(x_y,\theta_y^1)s^+(u,\theta_u)] - \gamma_f x_f \\
\dot{x}_g &= \kappa_g^1[1 - s^+(x_g,\theta_g^2)s^-(x_t,\theta_t^1)]s^-(x_f,\theta_f^4) - \gamma_g x_g \\
\dot{x}_t &= \kappa_t^1 s^+(x_g,\theta_g^2)s^-(x_t,\theta_t^1)s^+(x_f,\theta_f^4) - \gamma_t x_t \\
\dot{x}_r &= \kappa_r^1 s^+(x_f,\theta_f^3) + \kappa_r^2 - \gamma_r x_r
\end{aligned}
$$

$$
\begin{aligned}
&0 < \theta_c^1 < \tfrac{\kappa_c^1}{\gamma_c} < \tfrac{\kappa_c^1+\kappa_c^2}{\gamma_c} < \theta_c^2 < \theta_c^3 < \tfrac{\kappa_c^1+\kappa_c^3}{\gamma_c} \\
&0 < \theta_y^1 < \tfrac{\kappa_y^1}{\gamma_y} < \theta_y^2 < \theta_y^3 < \tfrac{\kappa_y^1+\kappa_y^2}{\gamma_y} \\
&0 < \theta_f^1 < \tfrac{\kappa_f^1}{\gamma_f} < \theta_f^2 < \theta_f^3 < \theta_f^4 < \theta_f^5 < \tfrac{\kappa_f^1+\kappa_f^2}{\gamma_f} \\
&0 < \theta_g^1 < \theta_g^2 < \tfrac{\kappa_g}{\gamma_g} \\
&0 < \theta_t^1 < \theta_t^2 < \tfrac{\kappa_t}{\gamma_t}
\end{aligned}
$$

Table 2: Attractors of Boolean model.

Att.	C_1	C_2	Y_1	Y_2	G_1	G_2	T_1	T_2	F_1	F_2	F_3	F_4
A1 ($U=1$)	1	1	1	$*$	1	$*$	0	0	0	0	0	0
A0 ($U=0$)	1	0	1	1	$*$	$*$	$*$	0	1	$*$	$*$	$*$

Since *rrn* is an output variable (it doesn't influence any of the other five), we will drop this variable and consider only four different thresholds for *fis*. Without loss of generality for the dynamics of the model, one can also say that *rrn* is activated once *fis* is above θ_f^2 (or θ_f^4). Therefore, we will assume that: $C,Y,G,T \in \{0,1,2\}$ and $F \in \{0,1,\ldots,4\}$.

To obtain the discrete model from the equations in Table 1, we follow the method indicated above. For example, consider the equation for x_c, which can take only one of four forms:

$$\dot{x}_c = \kappa_c^1 - \gamma_c x_c \quad (5)$$
$$\dot{x}_c = \kappa_c^1 + \kappa_c^2 - \gamma_c x_c \quad (6)$$
$$\dot{x}_c = \kappa_c^1 + \kappa_c^3 - \gamma_c x_c. \quad (7)$$
$$\dot{x}_c = \kappa_c^1 + \kappa_c^2 + \kappa_c^3 - \gamma_c x_c \quad (8)$$

For any state $V \in \Omega_d$, consider the appropriate equation (5)-(8), together with the inequalities in Table 1. In cases (5), (6): $C^+ = C+1$ if $C=0$, $C^+ = C$ if $C=1$, and $C^+ = C-1$ if $C=2$. In cases (7), (8): $C^+ = C+1$ if $C<2$, and $C^+ = C$ if $C=2$. The discrete transition tables can be found in the Supplementary Material. As an example, the table for *cya* is included in Appendix 2.

Following the method described in Section 2.1, Boolean rules for the *E. coli* network were constructed (see Supplementary Material). Analysis of this Boolean model shows that it has two attractors: a strongly connected component with four states when $U=1$, and a strongly connected component with 24 states in the case $U=0$. In Table 2, the fixed coordinates for each attractor are indicated. Following the method used in Tournier and Chaves (2009), it is possible to computationally identify the "operational interactions" within this attractor, and the variables associated with these interactions. That will give a subsystem of the original system.

For attractor A1 ($U=1$), we obtain: $G_2^+ = \overline{G_2}$ and $Y_2^+ = \overline{Y_2}$. That is, keeping one of the two variables G_2 or Y_2 fixed, the other can switch between zero and one, generating a fully reversible cycle, $00 \leftrightharpoons 10 \leftrightharpoons 11 \leftrightharpoons 01 \leftrightharpoons 00$. (see interpretation in Section 5).

For the attractor A0 ($U=0$), the operational subnetwork is depicted in Fig. 2. Several cycles are possible within attractor A0. The corresponding transition graph is represented in Figs. 4(a) ($T_1=0$) and 4(b) ($T_1=1$), and discussed in Section 4.

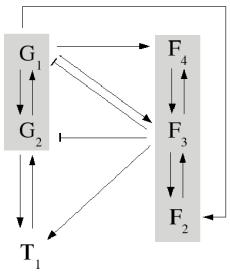

$$G_1^+ = \overline{F_3} \vee G_2$$
$$G_2^+ = \overline{F_3} \wedge G_1 \wedge (\overline{G_2} \vee T_1)$$
$$T_1^+ = F_3 \wedge G_2 \wedge \overline{T_1}$$
$$F_2^+ = G_1 \vee F_3$$
$$F_3^+ = (G_1 \vee F_4) \wedge F_2$$
$$F_4^+ = G_1 \wedge F_3 \wedge \overline{F_4}.$$

Figure 2: Operational interactions within attractor A0. Shaded regions indicate Boolean variables related to the same discrete multi-valued variable.

4 Comparison between Boolean and PWA differential models

To compare the two modelling formalisms, we now briefly summarize the results obtained in Grognard et al (2007) for the model in Table 1, for all sets of parameters satisfying the given inequalities. First, the solutions

were defined with the help of Filippov's differential inclusions. Then, the asymptotic dynamics were computed for the two values of the input. This system exhibits both equilibria (some in the sense of Filippov) and sliding modes. The latter is a type of solution where one of the variables is fixed at its threshold, for instance $x_i(t) = \theta_i^j$ for some i and j, and for t in some interval, while the other variables follow their vector fields. Even though the PWA system is not defined at thresholds, using Filippov's method, under some conditions it is possible to define a special type of solution (see Gouzé and Sari (2002) for more details). In practice (or in numerical simulations), this sliding motion may give rise to a rapid oscillatory behaviour of the variable x_i around its threshold θ_i^j, a phenomenon also called "chattering".

For the case $U = 1$, the asymptotic dynamics of the system in Table 1 satisfies:

- $x_c(t) \to \frac{\kappa_c^1+\kappa_c^2+\kappa_c^3}{\gamma_c} > \theta_c^3 > \theta_c^2$;
- $x_y(t) = \theta_y^3$, in finite time;
- $x_f(t) \to 0$;
- $x_g(t) = \theta_g^2$, in finite time;
- $x_t(t) \to 0$.

Therefore, solutions converge to an equilibrium point in the sense of Filippov. In practice, there is are sliding modes along $x_g = \theta_g^2$, and along $x_y(t) = \theta_y^3$. This characterization is obtained also with the Boolean model which, for the case $U = 1$, converges to attractor A1. In A1 only the values of $G_2 \in \{0,1\}$ and $Y_2 \in \{0,1\}$ may vary, and the transitions indeed correspond to a chattering mode in the variables x_g and/or x_y, between the highest ($G_1 = G_2 = 1$ or $Y_1 = Y_2 = 1$) and intermediate ($G_1 = 1$, $G_2 = 0$ or $Y_1 = 1$, $Y_2 = 0$) levels (see also Fig. 5(a)). The variables $C_1 = C_2 = 1$ indicate that x_c converges to its highest level, and also $T_{1,2} = 0$, $F_{1,2,3,4} = 0$, exactly recovering the piecewise affine asymptotic results for x_t and x_f.

For the case $U = 0$, the asymptotic dynamics of the system in Table 1 can be reduced to the equations on x_g and x_f (see Fig. 3) with:

- $x_c(t) \to \frac{\kappa_c^1}{\gamma_c}$ and $x_y(t) \to \frac{\kappa_y^1+\kappa_y^2}{\gamma_y}$, after some finite time;
- $x_t(t) \leq \theta_t^1$ and $x_g(t) \leq \theta_g^2$, after some finite time;
- Sliding mode along the plane $x_t = \theta_t^1$ with the solution eventually jumping down to the region $x_t < \theta_t^1$, and staying there;
- Sliding mode along the line $x_g = \theta_g^2$ and $x_f < \theta_f^4$, with the solution reaching (and leaving) the point $x_g = \theta_g^2$ and $x_f = \theta_f^4$ in finite time;
- Sliding mode along the line $x_g > \theta_g^1$ and $x_f = \theta_f^5$, with the solution reaching (and leaving) the point $x_g = \theta_g^1$ and $x_f = \theta_f^5$ in finite time;
- Damped oscillations around the point $x_g = \theta_g^1$ and $x_f = \theta_f^4$. It is shown that all trajectories will asymptotically converge to this point, which is an equilibrium in the sense of Filippov.

The interaction graph of the asymptotic system (x_f, x_g, x_t) obtained in Grognard et al (2007) (see also the diagram analysis in Tournier and Gouzé (2008)), is recovered in the diagram of operational interactions in Fig. 2. This graph has one negative loop between G and F, and two positive loops of length 2 and 3. The Boolean model correctly predicts the levels for x_c (intermediate, with $C_1 = 1$, $C_2 = 0$) and x_y (highest, with $Y_1 = 1$, $Y_2 = 1$). The Boolean model also predicts the three sliding modes: the transitions between states 000:110⇋000:100 or 100:110⇋100:100 (Fig. 4(a)), describe a possible chattering behaviour in variable G, which recovers the sliding mode along the line $x_g = \theta_g^2$. Similarly, the sliding mode along $x_f = \theta_f^5$ is recovered, with the transitions between states 110:110⇋111:110 or 110:100⇋111:100. Finally, from every state with $T_1 = 1$, a transition is possible to the corresponding state with $T_1 = 0$, i.e.: abc.de1→abc.de0. This transition is possible in both senses for the states: 110:111⇋110:110 and 111:111⇋111:110 (the states marked with $*$ in Figs. 4(a) and 4(b)). This captures the fact that eventually $x_t \leq \theta_t^1$, together with the sliding mode along $x_t = \theta_t^1$. For the oscillations in x_f, x_g, the

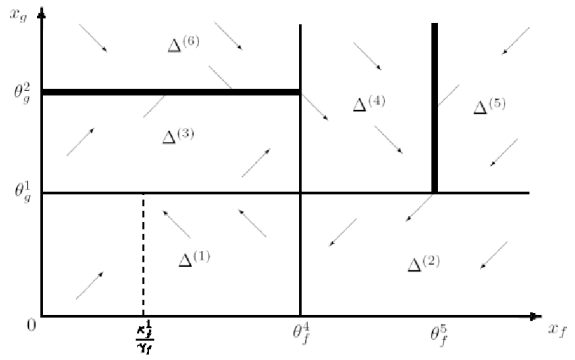

Figure 3: Asymptotic behaviour of the PWA in the (x_f, x_g) plane, for the case $U = 0$. Thick black lines indicate sliding modes (cf Grognard et al (2007)).

$$
\begin{array}{ccccccc}
000{:}110 & \rightarrow & 100{:}110 & \rightarrow & 110{:}110^* & \leftrightarrows & 111{:}110^* \\
\downarrow\uparrow & & \downarrow\uparrow & & \downarrow & & \downarrow \\
000{:}100 & \rightarrow & 100{:}100 & \rightarrow & 110{:}100 & \leftrightarrows & 111{:}100 \\
\uparrow & & \uparrow & & \downarrow & & \downarrow \\
000{:}000 & \leftarrow & 100{:}000 & \leftarrow & 110{:}000 & \leftarrow & 111{:}000
\end{array}
$$

(a)

$$
\begin{array}{ccccccc}
000{:}111^* & \rightarrow & 100{:}111^* & \rightarrow & 110{:}111^* & \leftrightarrows & 111{:}111^* \\
\uparrow & & \uparrow & & \downarrow & & \downarrow \\
000{:}101^* & \rightarrow & 100{:}101^* & \rightarrow & 110{:}101^* & \leftrightarrows & 111{:}101^* \\
\uparrow & & \uparrow & & \downarrow & & \downarrow \\
000{:}001^* & \leftarrow & 100{:}001^* & \leftarrow & 110{:}001^* & \leftarrow & 111{:}001^*
\end{array}
$$

(b)

Figure 4: Transition graph within attractor A0, for $T_1 = 0$ (a) and $T_1 = 1$ (b). The state 110:101 represents: $(F_2, F_3, F_4) = (1,1,0)$ and $(G_1, G_2, T_1) = (1,0,1)$. The star indicates a possible transition to the corresponding state with opposite T_1.

Boolean model predicts the same orientation as that of the PWA model (compare Figs. 4(a) and 3). Note that these figures can be read as a "phase portrait" of the system, with the period two oscillations corresponding to the dark solid lines in Fig. 3.

In summary, all the main qualitative asymptotic properties of the PWA system are recovered in its Boolean counterpart, but some fine-grained aspects of the dynamics are lost. Even though the phase portraits in both formalisms are identical from a qualitative point of view, the Boolean model loses the fact that the oscillations are damped, and that the trajectories eventually converge to a fixed point in the sense of Filippov. In Grognard et al (2007), the demonstration of this convergence was made through a fine analysis of the sliding modes and computation of a Poincaré map. The Boolean model also loses the information that the lines $x_g = \theta_g^2$ or $x_f = \theta_f^5$ (bold lines in Fig. 3) are in fact "black walls", which effectivelly prevent trajectories to cross from one side to the other. This information is, however, only hidden in the Boolean framework and can be uncovered by finer modelling, to recover the convergence towards singular domains, as shown in the next Section.

5 Sliding modes and period two Boolean oscillations

The attractors of a Boolean model describe the possible asymptotic behaviours of the network and depend on the model's size, connectivity, and rules. The attractors in a given network can be counted and classified according to its qualitative dynamical properties (Bagley and Glass, 1996) but, however, not all attractors represent biologically relevant or even observed behaviour. In our example, we observe several short one-step cycles where the system may be locked in a period 2 oscillation that might constitute suspicious non-biological behaviour. Nevertheless, in this case, comparison with the PWA model shows that *all the one-step oscillations* correspond

to a given "sliding mode" in the continuous system. The biological significance of these sliding motions can be related to the phenomenon of homeostasis, where the regulatory network contributes to maintain a biological species around a given level.

Assume that the Boolean model dynamics has a period 2 oscillation in variable i, whenever the system is in a subset $R^b \in \Omega$:

$$X_i^+ = F_i(X) = \overline{X_i} = \begin{cases} 0, & X_i = 1,\ X \in R^b \\ 1, & X_i = 0,\ X \in R^b. \end{cases} \tag{9}$$

The smallest possible set $R^b = \{X^0, X^1\}$, is such that $X_i^0 = 0 = 1 - X_i^1$, and $X_j^0 = X_j^1$ for all $j \neq i$. Recall that $X_i = 1$ (resp., $X_i = 0$) means that a biological variable x_i is above (resp., below) its threshold value θ_i. We next show the correspondence between Boolean model (9), which oscillates between the two states "above" and "below" the threshold, and a PWA system that exhibits a sliding mode solution $x_i(t) \equiv \theta_i$. In fact, this correspondance illustrates the "chattering" phenomenon: if the real system can only distinguish a small number of qualitative states ("above" and "below" the threshold), then the *closest* way to represent a solution of the form $x_i(t) \equiv \theta_i$ is to repeateadly switch back and forth between the two qualitative states, thus passing repeatedly through the point θ_i.

Consider a region R of the (continuous) state space corresponding to R^b, where variable x_i may cross a threshold value but all other x_j ($j \neq i$) are in a interval between two thresholds:

$$R = \{x \in \mathbb{R}^n_{\geq 0} : \text{sign}(X_j - 1/2)x_j > \theta_j,\ \theta_i - \varepsilon < x_i < \theta_i + \varepsilon\}.$$

Assume further that $\text{sign}(f_j(x))$ =const. for all $x \in R$, $j \neq i$. Following (9) and (4), the PWA equation for x_i must satisfy:

$$\dot{x}_i = f_i(x) \begin{cases} < 0, & x_i > \theta_i, x \in R \\ \text{any}, & x_i = \theta_i, x \in R \\ > 0, & x_i < \theta_i, x \in R \end{cases}$$

A simple PWA system that satisfies these properties is of the form

$$\begin{aligned} \dot{x}_i &= f_i(x) = \kappa_i s^-(x_i, \theta_i) - \gamma_i x_i, \quad x \in R, \\ \dot{x}_j &= f_j(x), \quad \text{has constant sign } \ \forall\, x \in R \quad (j \neq i) \end{aligned}$$

with a negative auto-regulatory function for i, and $\theta_i < \kappa_i/\gamma_i$. This system admits no equilibrium with $x_i \neq \theta_i$ (since $f_i(x) \neq 0$), but it admits an equilibrium of Filippov type: $\hat{x}_i = \theta_i$. It is clear that, in R, x_i will approach the point θ_i in finite time (because $\kappa_i/\gamma_i > \theta_i$, and $x_i(t) = (x_i(0) - \kappa_i/\gamma_i)e^{-\gamma_i t} + \kappa_i/\gamma_i$ for $x_i(0) < \theta_i$, and $x_i(t) = x_i(0)e^{-\gamma_i t}$ for $x_i(0) > \theta_i$). Assume that the system evolves in R until the variable x_i reaches its threshold θ_i, at some instant T_1. This gives rise to a "sliding mode" solution on R, since $x_i(t) = \theta_i$ for t in some interval $[T_1, T_2]$, while the other variables increase or decrease until the trajectory leaves R at $t = T_2 > T_1$. In theory, we expect no oscillations in x_i, even if, due to the discontinuity in the vector field, numerical simulations may show oscillations. A comparison can be made with the solution of a continuous vector field $\dot{x}_i = \kappa_i \theta_i^p/(\theta_i^p + x_i^p) - \gamma_i x_i$ ($p \geq 2$), which has a single stable equilibrium, and no damped oscillations.

This correspondence between period 2 oscillations and sliding modes can be further interpreted as follows: the "back-and-forth" oscillatory behaviour may be the result of the existence of an intermediate variable which is lacking in the Boolean model. So, introduce a new variable associated with x_i as follows: $X_{i*} = 0$ if $x_i < \theta_i$ and $X_{i*} = 1$ if $x_i \geq \theta_i$. In order to define the Boolean dynamics, we construct the following table:

x_i	X_{i*}	X_i	X_{i*}^+	X_i^+
$< \theta_i$	0	0	1	0
$= \theta_i$	1	0	1	0
$> \theta_i$	1	1	1	0

The first and third line are straightforward. The second line is interpreted like this: when $(X_{i*}, X_i) = (1,0)$, i.e. when $x_i = \theta_i$, then the two neighbor vector fields are of opposite sign, and therefore force the variable x_i to remain constant.

To illustrate this, consider the attractor A1, consisting of the reversible transitions in a 2 dimensional space G_2Y_2. Note that, fixing either of the variables, the other may have a period 2 oscillation. Introducing one intermediate variable for each of G_2 and Y_2, the attractor A1 expands to the form shown in Fig. 5(b) (with notation $G_{2*}G_2 : Y_{2*}Y_2$). This diagram represents exactly the Filippov type equilibrium for the case $U = 1$, where $x_g \to \theta_g^2$ and $x_y \to \theta_y^3$ in finite time. In the Boolean model, both one-step oscillations disappear, and the strongly connected component containing four states is "decoupled", giving rise to a Boolean steady state: $G_{2*}^+ = 1$, $G_2^+ = 0$, $Y_{2*}^+ = 1$, and $Y_2^+ = 0$.

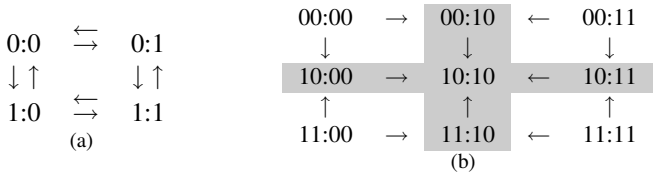

Figure 5: (a) Transition graph within attractor A1. The state 1:0 represents: $(G_2 : Y_2) = (1 : 0)$. (b) Resolving the "chattering" behaviour in attractor A1, by adding intermediate variables. The state 10:00 represents: $(G_{2*}G_2 : Y_{2*}Y_2) = (10 : 00)$.

6 Conclusions

Two formalisms, Boolean and piecewise affine models, were compared in this paper. The analysis shows that the Boolean model captures most of the asymptotic behaviour of the system, even though the PWA model gives more details. Namely, the Boolean model correctly reproduces oscillatory behaviour and sliding modes, but it cannot capture convergence to a given point through damped oscillations, or the fact that a sliding mode along a given line plays the role of a black wall. This latter problem can be circumvented by noticing that there is a correspondence between sliding modes and period 2 Boolean cycles, and adding a new variable to more finely describe the local oscillatory behaviour. Therefore, dynamical behaviour in the Boolean model that might be considered as non-relevant biologically may in fact contain useful information for analysis of complex systems.

Moreover, for the *E. coli* network, we have been able to identify a Boolean subsystem corresponding to each attractor of the full Boolean system. In our case, the dynamics of this asymptotic Boolean system was compared to the computed asymptotic dynamics of the differential system, and shown to be very similar. More generally, this reduced Boolean asymptotic system could be again translated into a continuous one, to obtain a reduced system of the full differential system, hopefully keeping some of the asymptotic properties of the full system. This offers interesting perspectives for model reduction.

Given the available computational tools for Boolean analysis, based on well known and efficient graph algorithms (see, for instance, Sánchez and Thieffry (2001); Ropers et al (2006); Tournier and Chaves (2009)), the construction of a Boolean model associated to a PWA system can therefore constitute an undeniable help for the analysis of genetic regulatory networks.

Acknowledgements

This work was supported in part by the French National Research Agency through the BioSys project MetaGenoReg.

References

Bagley R, Glass L (1996) Counting and classifying attractors in high dimensional dynamical systems. J Theor Biol 183:269–284

Casey R, de Jong H, Gouzé J (2006) Piecewise linear models of genetic regulatory networks: equilibria and their stability. J Math Biol 52:27–56

Chaves M, Sontag E, Albert R (2006) Methods of robustness analysis for boolean models of gene control networks. IEE Proc Systems Biology 235:154–167

Chaves M, Eißing T, Allgöwer F (2009) Regulation of apoptosis via the nfkb pathway: modeling and analysis. In: N Ganguly AD, Mukherjee A (eds) Dynamics on and of complex networks: applications to biology, computer science and the social sciences, Modeling and Simulation in Science, Engineering and Technology, Birkhauser, Boston, pp 19–34

von Dassow G, Meir E, Munro E, Odell G (2000) The segment polarity network is a robust developmental module. Nature 406:188–192

Glass L (1975) Classification of biological networks by their qualitative dynamics. J Theor Biol 54:85–107

Glass L, Kauffman S (1973) The logical analysis of continuous, nonlinear biochemical control networks. J Theor Biol 39:103–129

Gouzé J, Sari T (2002) A class of piecewise linear differential equations arising in biological models. Dyn Syst 17(4):299–316

Grognard F, Gouzé JL, de Jong H (2007) Piecewise-linear models of genetic regulatory networks: theory and example. In: Queinnec I, Tarbouriech S, Garcia G, Niculescu S (eds) Biology and control theory: current challenges, Lecture Notes in Control and Information Sciences (LNCIS) 357, Springer-Verlag, pp 137–159

van Ham P (1979) How to deal with more than two levels. In: Thomas R (ed) Kinetic Logic: A Boolean Approach to the Analysis of Complex Regulatory Systems, Lecture Notes in Biomathematics, vol 29, Springer, pp 326–343

Liang S, Fuhrman S, Somogyi R (1998) REVEAL, a general reverse engineering algorithm for inference of genetic network architecture. In: Pacific Symposium on Biocomputing, vol 3, pp 18–29

Ropers D, de Jong H, Page M, Schneider D, Geiselmann J (2006) Qualitative simulation of the carbon starvation response in *Escherichia coli*. Biosystems 84(2):124–152

Sánchez L, Thieffry D (2001) A logical analysis of the *Drosophila* gap-gene system. J Theor Biol 211:115–141

Snoussi E, Thomas R (1993) Logical identification of all steady states: the concept of feedback loop characteristic states. Bull Math Biol 55(5):973–991

Thomas R, D'Ari R (1990) Biological feedback. CRC Press

Tournier L, Chaves M (2009) Uncovering operational interactions in genetic networks using asynchronous boolean dynamics. J Theor Biol 260(2):196–209

Tournier L, Gouzé JL (2008) Hierarchical analysis of piecewise affine models of gene regulatory networks. Theory Biosci 127:125–134

Zhang J, Johansson K, Lygeros J, Sastry S (2001) Zeno hybrid systems. Int J Robust Nonlinear Control 11:435–451

APPENDIX

1 Discrete (multi-level) and Boolean

We now sketch an intuitive algorithm that always provides a biologically feasible model consistent with the multi-level one. Our construction is based on the hypotheses H1 and H2, stated in Section 2.1

Given a discrete model $\Sigma_d = (\Omega_d, F_d)$, with variables $V = (V_1, \ldots, V_M)$ and state space $\Omega_d = \{0, 1, \ldots, d_1\} \times \cdots \times \{0, 1, \ldots, d_M\}$ let $F_d(V)$ denote the synchronous successor of V and $V[t+1] = F_{d,asyn}(V[t])$ represent the asynchronous dynamics, where $F_{d,asyn}(V)$ takes values in the set (1).

Assume that each of the M discrete variables has d_m ($m = 1,\dots,M$) levels and define: $D = (d_1,\dots,d_M)$, $n = d_1 + \cdots + d_M$ and set $\Omega = \{0,1\}^n$. Then define a function $\varphi_D : \Omega_d \to \Omega$, such that:

$$\varphi_D(V) = (V_{1,1},\dots,V_{1,d_1},\dots,V_{M,1},\dots,V_{M,d_M}), \tag{10}$$

where $V_{m,k}$ are defined as in (2). It is clear that the function is injective, but $\varphi_D(\Omega_d)$ is strictly contained in Ω. Namely, those elements of Ω that would satisfy $V_{m,k} < V_{m,k+1}$ for some m and some $1 \le k \le d_m$ do not have a pre-image in Ω_d. In fact, such combinations are biologically meaningless, in view of the interpretation of (2). Moreover, when constructing the Boolean rules for the extended system, one naturally wishes to avoid transitions to these unfeasible states, in order to obtain a biologically significant model. Define the sets of *permissible* and *forbidden* states of Ω, associated with D:

$$\begin{aligned} S_{D,p} = &\quad \{X \in \Omega :\ (\forall\ 1 \le m \le M)(\forall\ 1 \le k \le d_m),\ X_{m,k} \ge X_{m,k+1}\} \\ S_{D,f} = &\quad \{X \in \Omega :\ (\exists\ 1 \le \bar{m} \le M)(\exists\ 1 \le \bar{k} \le d_{\bar{m}}),\ X_{\bar{m},\bar{k}} < X_{\bar{m},\bar{k}+1}\}, \end{aligned}$$

where the n coordinates of vector $X \in \Omega$ are labelled in M groups of length d_m:

$$X = (X_{1,1},\dots,X_{1,d_1},\dots,X_{M,1},\dots,X_{M,d_M}). \tag{11}$$

Note that: $S_{D,p} = \varphi_D(\Omega_d)$ and $S_{D,f} = \Omega \setminus S_{D,p}$, in view of H2. Then φ_D is a bijection between Ω_d and $S_{D,p}$, so it is possible to define a (partial) inverse function:

$$\varphi_{D,p}^{-1} : S_{D,p} \to \Omega_d, \quad \varphi_{D,p}^{-1}(X) = (V_1,\dots,V_M),$$

where $V_m = \sum_k X_{m,k}$. An algorithm for generating a Boolean model $\Sigma_b = (D,\Omega,F_b)$ associated to Σ_d is then as follows:

1. Generate the state space: $\Omega = \{0,1\}^n$ with $n = d_1 + \cdots + d_M$, and label the coordinates of $X \in \Omega$ according to (11);
2. Translate the discrete value table $F_d(V)$ into a Boolean value table $F_b(X)$, for each $X \in S_{D,p}$:

   $$F_b(X) := \varphi_D(F_d(V)) = \varphi_D(F_d(\varphi_{D,p}^{-1}(X)))$$

   (note that this assigns values to $X \in S_{D,p}$ only);
3. Complete the table F_b by assigning any function $\psi : \Omega \to \Omega$ to the Boolean states $X \in S_{D,f}$:

   $$F_b(X) = \begin{cases} \varphi_D(F_d(\varphi_{D,p}^{-1}(X))), & X \in S_{D,p} \\ \psi(X), & X \in S_{D,f}; \end{cases}$$

4. Obtain Boolean logical rules from the (now full) synchronous truth table F_b.

Note that step 3 can be viewed as the identification of a n-dimensional Boolean map, verifying certain constraints (on the set $S_{D,p}$) and with some degrees of freedom (on the set $S_{D,f}$). Thus the map $F_b : \Omega \to \Omega$ is not necessarily unique. To construct this map, one can use a reverse engineering algorithm, to find a function ψ according to some suitable criteria (for instance, REVEAL Liang et al (1998) will find a function ψ with minimal node connectivity). In any case, the values of $F_b(S_{D,f})$ *will not affect the dynamics of the biologically relevant part of the Boolean model*. Lemma 1 shows that the Boolean model thus obtained is well defined and biologically consistent with the discrete model, in the sense that no forbidden state will be a successor of a permissible state. Forbidden states can succeed one another or go into a permissible state. (Grey rows in Table 3)

For the Boolean model $\Sigma_b = (D,\Omega,F_b)$, one can also define an asynchronous dynamics from F_b, by updating only one Boolean variable at a time, $X[t+1] = F_{b,asyn}(X[t])$. Note that synchronous and asynchronous dynamics have the same equilibrium points: $X^+ = F_b(X) = X$ implies $X[t+1] = X[t]$ for all t.

Lemma 1 *Suppose Σ_d is a multi-level system that satisfies H1. The Boolean system $\Sigma_b = (D,\Omega,F_b)$, constructed according to H2 and points 1 to 3, allows only transitions from $S_{D,p}$ or $S_{D,f}$ into $S_{D,p}$ or from $S_{D,f}$ into itself (for both synchronous and asynchronous updating strategies).*

Proof: Given any $X \in S_{D,p}$, we want to show that $X^+ = F_b(X) \in S_{D,p}$. By definition of F_b, φ_D and $\varphi_{D,p}^{-1}$ we have:

$$F_b(X) = \varphi_D(F_d(\varphi_{D,p}^{-1}(X))) = \varphi_D(F_d(V)) = \varphi_D(V^+),$$

for some $V \in \Omega_d$. By assumption H2, it follows that $\varphi_D(V^+) \in S_{D,p}$.

The forbidden states can remain in $S_{D,f}$ or switch to $S_{D,p}$ since, given any $X \in S_{D,f}$, we have $X^+ = F_b(X) = \psi(X)$ and $\psi(X) \in \Omega = S_{D,p} \cup S_{D,f}$. To see that the asynchronous updating strategy also prevents transitions from $S_{D,p}$ to $S_{D,f}$, consider $X \in S_{D,p}$ and any asynchronous transition, $Y = F_{b,asyn}(X)$. If X is an equilibrium point then immediately $Y = X \in S_{D,p}$. Otherwise, since X is of the form (10), it can be written as: $X = (\vec{1}_{p_1}, \vec{0}_{d_1-p_1}; \cdots; \vec{1}_{p_M}, \vec{0}_{d_M-p_M})$, where $\vec{1}_p$ (resp., $\vec{0}_p$) is a vector of length p with all coordinates equal to 1 (resp., 0). Its synchronous successor is $X^+ = (\vec{1}_{p_1^+}, \vec{0}_{d_1-p_1^+}; \cdots; \vec{1}_{p_M^+}, \vec{0}_{d_M-p_M^+})$, where $p_i^+ \in \{p_i - 1, p_i, p_i + 1\}$, for all $i = 1, \ldots, M$. Since X is not an equilibrium point, then there exists $k \in \{1, d_M\}$ such that $p_k^+ \neq p_k$. In any asynchronous successor, only one p_i can change at a time. Therefore, there exists exactly one index $1 \leq k \leq M$ such that $p_k^+ = p_k \pm 1$: $Y = (\vec{1}_{p_1}, \vec{0}_{d_1-p_1}; \cdots; \vec{1}_{p_k^+}, \vec{0}_{d_1-p_k^+}; \cdots; \vec{1}_{p_M}, \vec{0}_{d_M-p_M})$. Therefore, it is clear that $Y \in S_{D,p}$. ∎

2 Multi-level and Boolean state transition tables for *cya*

To illustrate the construction of the Boolean rules from the piecewise affine model, we now give the complete tables for the variable *cya*. The rules for the other variables can be similarly obtained (the full tables can be found in the Supplementary Material). The left panel in Table 3 shows the multi-level model rules for *cya*, in the cases $U = 0$ or $U = 1$. The columns C and Y contain the multi-level states corresponding to the (continuous) variables x_c and x_y, obtained by application of (3). The column Y^+ shows the synchronous state transition, computed according to (4). Columns Y_1^+ and Y_2^+ depict the states of the Boolean variables corresponding to Y^+, computed according to hypotheses H1 and H2. The right panel in Table 3 shows the Boolean variables corresponding to C and Y in the first four columns, and the synchronous Boolean updates in the columns Y_1^+ and Y_2^+. As explained in the text, there are Boolean state combinations which have no biological meaning: these are the rows highlighted in grey and represent the forbidden states in $S_{D,f}$. The corresponding entries in columns Y_1^+ and Y_2^+ are filled following points 1 to 3, in Appendix 1. Therefore, according to Lemma 1, there are no transitions to forbidden states. The Boolean rules for *cya* can be now read from the columns C_i, Y_i, and Y_i^+:

$$\begin{aligned} Y_1^+ &= 1 \\ Y_2^+ &= (\overline{U} \wedge Y_1) \vee (U \wedge [(Y_1 \wedge (\overline{C_1} \vee \overline{C_2})) \vee ((Y_1 \wedge \overline{Y_2}) \wedge C_1 \wedge C_2)]) \end{aligned}$$

Table 3: Multi-level model and Boolean rules for *cya* (Y) (synchronous maps F_d and F_b).

C	Y	U	Y^+	Y_1^+	Y_2^+
0	0	0 1	1 1	1 1	0 0
0	1	0 1	2 2	1 1	1 1
0	2	0 1	2 2	1 1	1 1
1	0	0 1	1 1	1 1	0 0
1	1	0 1	2 2	1 1	1 1
1	2	0 1	2 2	1 1	1 1
2	0	0 1	1 1	1 1	0 0
2	1	0 1	2 2	1 1	1 1
2	2	0 1	2 1	1 1	1 0

C_1	C_2	Y_1	Y_2	U	Y_1^+	Y_2^+
0	0	0	0	0 1	1 1	0 0
0	0	0	1	0 1	1 1	0 0
0	0	1	0	0 1	1 1	1 1
0	0	1	1	0 1	1 1	1 1
0	1	0	0	0 1	1 1	0 0
0	1	0	1	0 1	1 1	0 0
0	1	1	0	0 1	1 1	1 1
0	1	1	1	0 1	1 1	1 1
1	0	0	0	0 1	1 1	0 0
1	0	0	1	0 1	1 1	0 0
1	0	1	0	0 1	1 1	1 1
1	0	1	1	0 1	1 1	1 1
1	1	0	0	0 1	1 1	0 0
1	1	0	1	0 1	1 1	0 0
1	1	1	0	0 1	1 1	1 1
1	1	1	1	0 1	1 1	1 0